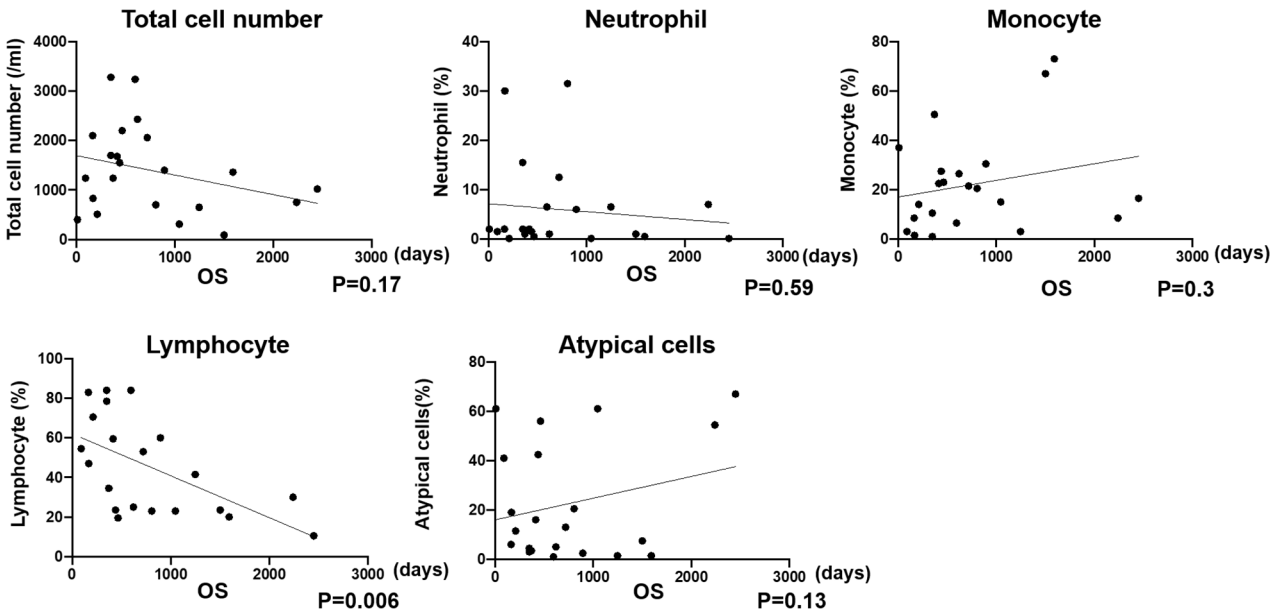

Figure S1 Correlation between OS and cell fractions in MPE. Linear correlation between OS and cell fractions in pleural effusion was evaluated based on Pearson's correlation coefficient in all eligible patients with NSCLC (n=22). OS, overall survival; MPE, malignant pleural effusion; NSCLC, non-small cell lung cancer.

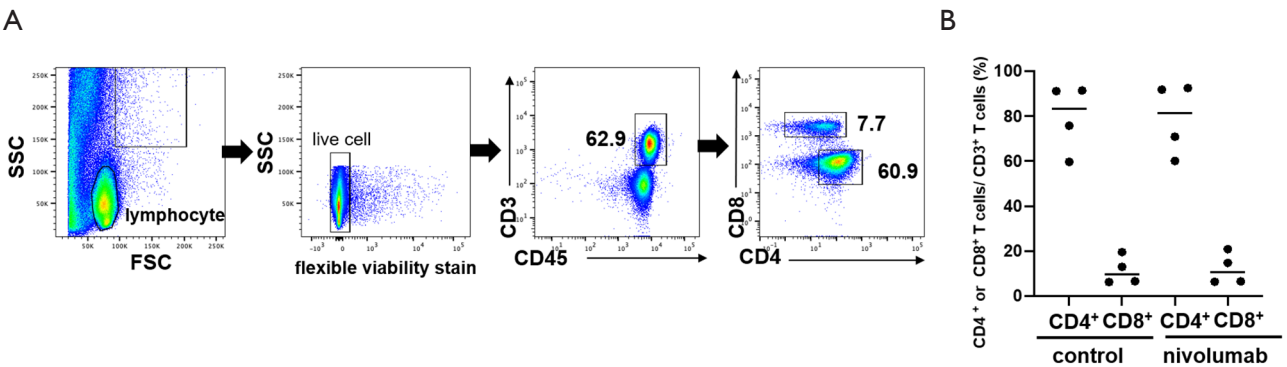

Figure S2 Gating strategy and proportion of $CD4^+$ and $CD8^+$ T cells in MPE. (A) Gating strategy of $CD4^+$ and $CD8^+$ T cell was shown. (B) Percentage of $CD4^+$, $CD8^+$ T cells in MPE. Four independent experiments were performed, and similar results were obtained. MPE, malignant pleural effusion; FCS, forward scatter; SSC, side scatter.

https://dx.doi.org/10.21037/tlcr-24-559

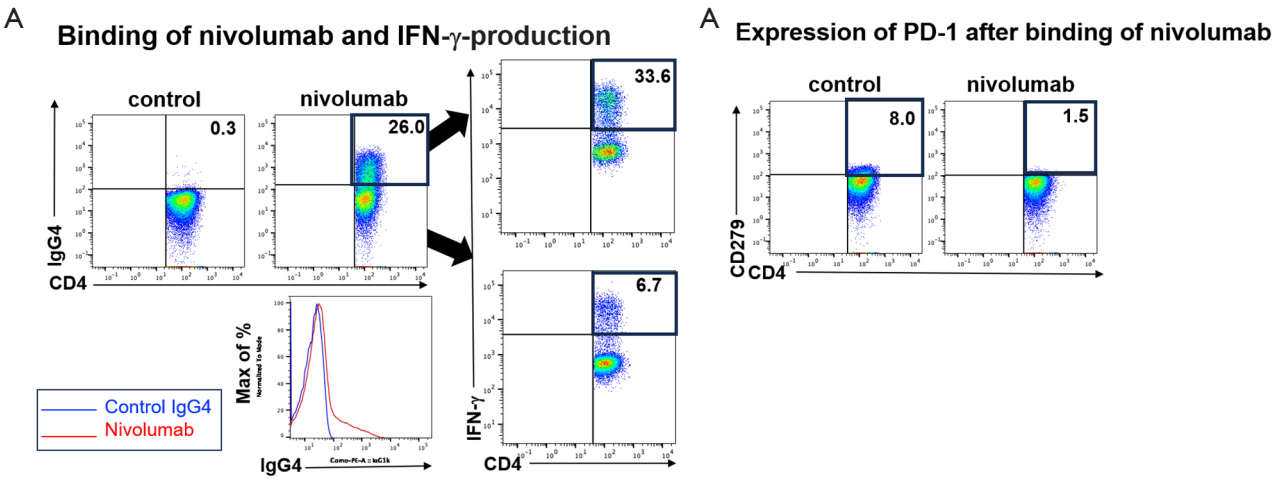

Figure S3 IFN-γ production from nivolumab-binding CD4⁺ T cells in the *in vitro* bioassay. Representative flow cytometry plots of CD4⁺ T cells in *in vitro* bioassay were depicted. (A) Whole-cell component of MPE was co-cultured with control IgG4 antibody or nivolumab, binding of these antibodies on CD4⁺ T cells were confirmed through staining with an anti-IgG4 antibody. Production of IFN-γ from T cells was evaluated by intracellular staining of IFN-γ. (B) The change of PD-1-expression on CD4⁺ T cells after binding of nivolumab was evaluated by anti-CD279 (PD-1) antibody. Four independent experiments were performed, and similar results were obtained. IFN-γ, interferon-gamma; IgG4, immunoglobulin G4; PD-L1, programmed cell death-ligand 1; MPE, malignant pleural effusion; interferon-gamma.

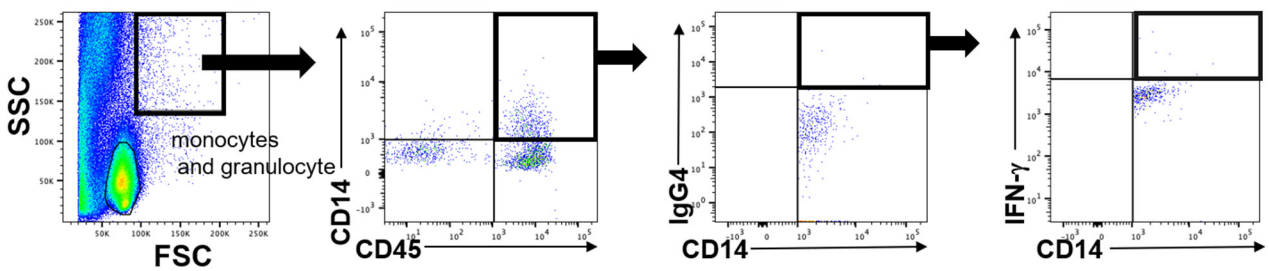

Figure S4 Analysis of monocytes in MPE. Gating strategy of monocyte in MPE was demonstrated. Representative flow cytometry plots are shown. FCS, forward scatter; SSC, side scatter; IgG4, immunoglobulin G4; IFN-γ, interferon-gamma; MPE, malignant pleural effusion.

https://dx.doi.org/10.21037/tlcr-24-559